

Effects of the intense solar activity of March/June 1991 observed in the outer heliosphere

F. B. McDonald,¹ A. Barnes,² L. F. Burlaga,³ P. Gazis,⁴ J. Mihalov,² and R. S. Selesnick⁵

Abstract. The properties of the large-scale global merged interaction region (GMIR) generated by the intense solar events of March and June 1991 are studied using the available solar wind, interplanetary magnetic field, and energetic particle data from the observing network of Pioneer 10 and Voyagers 1 and 2 in the outer heliosphere. At heliocentric distances extending to 55 AU the delayed effects of this enhanced solar activity are observed in the form of large increases in the solar wind velocity and interplanetary magnetic field and significant decreases in the galactic cosmic ray intensity. For low-energy ions (5-MeV protons) there was a single long-lived event extending over a period of some 6 months. Near the strongest interplanetary disturbances the H and He spectra are best represented by similar exponentials in momentum/nucleon (i.e., particle velocity at these energies). Over the rest of the event the characteristic momentum for He, $(P_0)_{\text{He}}$ is generally ~ 0.66 for hydrogen. These spectra and the consistently low H/He ratio (25.3) at 2 MeV/nucleon closely resemble that observed in corotating interaction regions events. Despite the strong north/south asymmetry in the solar activity, the interplanetary disturbances produced the same net decrease in the galactic cosmic ray intensity of ions >70 MeV at the three widely separated spacecraft when the effects of the long-term recovery are taken into account. A comparison of the relative intensity of MeV ions at these three spacecraft suggest that the most intense solar events occurred on the back side of the Sun in time periods adjacent to the March and June episodes of solar activity. It is argued that this GMIR as a system is responsible for the low-frequency radio emission observed by the Voyager Plasma Wave experiment some 1.46 years after the onset of the March 1991 activity.

1. Introduction

In December 1990, some 17 months after the time of maximum solar activity in cycle 22, there began a new increase in activity that culminated with 35 major flares (X ray classification M-5 or higher) in March 1991, with most of these events coming from three regions in the Sun's southern hemisphere. The next 2 months were relatively quiet, but in June the premiere active region of cycle 22 appeared in the Sun's northern hemisphere, producing in a single passage 6 x class flares, 5 of which saturated the GOES X ray detectors. Major solar energetic particle events and large Forbush decreases were observed in association with some of the more intense of these solar outbursts.

In the outer heliosphere, experiments on the Pioneers 10

and 11 and Voyagers 1 and 2 spacecraft at heliocentric distances ranging from 34 to 52 AU observed the delayed effect of this enhanced solar activity in the form of several large increases in the solar wind velocity and interplanetary magnetic field, significant decreases in the galactic cosmic ray intensity, and, for low-energy ions (5-MeV protons) there was a long-lived event extending over a period of some 6 months. These low-energy particles mark the passage of the large-scale interplanetary structure that had evolved with increasing heliocentric distance.

Such long-lived increases in the flux of MeV ions in the outer heliosphere have been observed previously [Van Allen and Mihalov, 1990; McDonald and Selesnick, 1991; Decker et al., 1991] and generally occur in conjunction with step decreases in the intensity of galactic and anomalous cosmic rays. These disparate changes in the low- and high-energy particle populations are associated with the passage of large-scale disturbances in the interplanetary medium known as global merged interaction regions (GMIRs). Originally identified by Burlaga et al. [1984, 1985, 1993], GMIRs form and evolve with increasing heliocentric distance through the coalescence of interplanetary shocks and interaction regions produced by coronal mass ejections and high-speed solar wind streams. These systems are a major element in producing the long-term 11-year cosmic ray modulation [Burlaga et al., 1991, 1993; Perko and Burlaga, 1992; le Roux and Potgieter, 1993; Potgieter, 1993; McDonald et al., 1993].

¹Institute for Physical Science and Technology, University of Maryland, College Park.

²Space Science Division, NASA Ames Research Center, Moffett Field, California.

³Laboratory for Extraterrestrial Physics, NASA Goddard Space Flight Center, Greenbelt, Maryland.

⁴San Jose State University, NASA Ames Research Center, Moffett Field, California.

⁵California Institute of Technology, Pasadena.

Copyright 1994 by the American Geophysical Union.

Paper number 94JA01004.
0148-0227/94/94JA-01004\$05.00

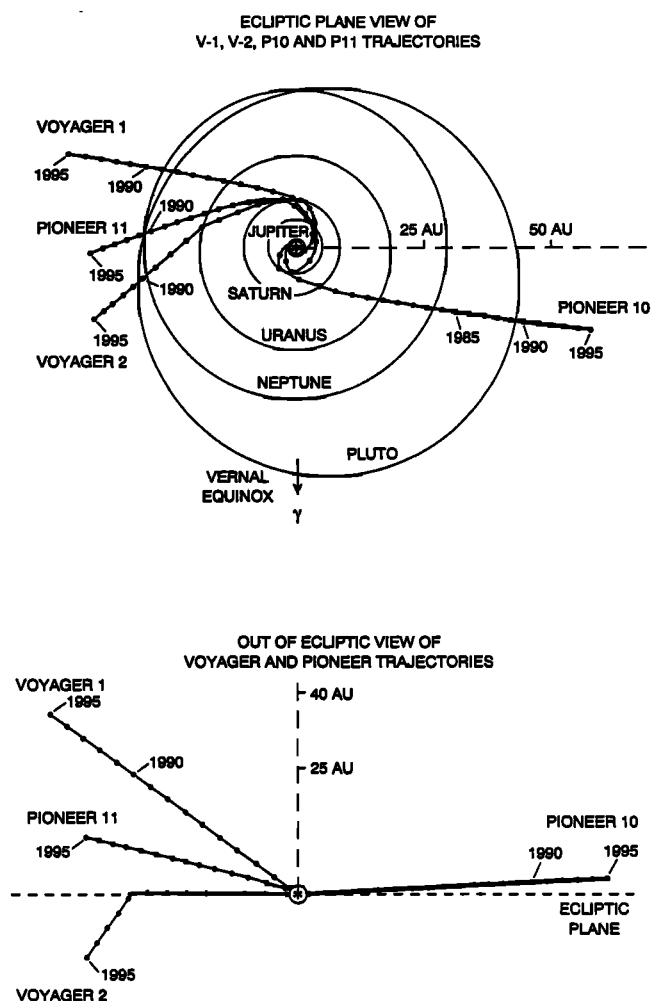


Figure 1. Ecliptic and out-of-the ecliptic plane projections of the Voyager 1 and 2 and Pioneers 10 and 11 trajectories from launch through the end of 1994.

The isolated occurrence in time of these major episodes of solar activity in March and June 1991, their north-south asymmetry, the large increase of low-energy ions and decreases in the galactic cosmic ray intensity in the outer heliosphere offer a unique opportunity to study the generation of a GMIR, its relation to events on the Sun, to the acceleration and transport of MeV ions, and to cosmic ray modulation. These questions are explored in this paper using the solar wind, interplanetary magnetic field, and energetic particle data available from the Pioneer and Voyager deep space missions, the IMP 8 energetic particle data from 1 AU and appropriate solar observations. Previously, *Van Allen and Fillius* [1992] and *Webber and Lockwood* [1993] have discussed the changes in the galactic cosmic ray intensity at the Voyagers and Pioneers over this same time period.

This particular GMIR takes on added importance with its role as the probable trigger for the strong outburst of low-frequency ($\sim 2\text{--}3$ KHz) radio emission observed by the Voyagers 1 and 2 Plasma Wave System (PWS) [*Gurnett et al.*, 1993] starting in mid-July 1992, more than a year after the leading edge of the GMIR passed V2 at 34.7 AU.

2. Observations

2.1. 1991 Spacecraft Locations

The propitious locations (Figure 1) of the four spacecraft in 1991 provide an excellent deep space network for studying the spatial and temporal variations of the large scale interplanetary disturbances and changes in the energetic particle population produced by the March/June activity. In mid-1991, P10 (52.4 AU) and V2 (35.3 AU) are near the plane of the ecliptic but separated by 153° in heliolongitude. V1 (45.8 AU) at a heliolatitude of $\lambda = 33^\circ\text{N}$ and P11 (33.6 AU), $\lambda = 17^\circ\text{N}$, extend a three-dimensional perspective to these studies.

2.2. Solar and 1 AU Observations

The major flares, as defined by their peak X ray emission in the $1\text{--}8 \text{ \AA}$ range, are taken as a proxy for the general level of solar activity. In Figure 2 the peak X ray emissions for events with an identifiable flare whose maximum X ray emission exceeded $5 \times 10^{-5} \text{ W/m}^2$ for $1\text{--}8 \text{ \AA}$ X rays at the GOES detector are plotted as a function of time with the $\pm y$ axis used to denote the north/south location of the flare. However, there is not a strong correlation between the size of the X ray flare emission and the existence and properties of coronal mass events (CMEs) [cf. *Kahler*, 1992], which are the principal agents, along with high-speed solar wind streams, for producing interplanetary disturbances. Those flare events that have an associated CME (as listed in Solar Geophysical Data) have a circle drawn around their peak value. The March CME-related events occur mainly in the southern hemisphere, and there is a broad distribution in the X ray flare size.

The June period is remarkably different. There are six very large events with a cluster of smaller events around the 10^{-5} W/m^2 level, all in the northern hemisphere. A surprising number of these June–July events have associated CMEs and the size distribution with the number of very large events and the paucity of smaller events is unusual. There is growing evidence that CMEs are not produced by the solar flare and in many cases are observed to precede the flare onset [cf. *Kahler*, 1992; *Gosling*, 1993]. However, these large June events typify what *Kahler* terms the “large flare syndrome” in which some of the very largest solar events are outstanding in essentially all aspects, including optical, X ray, γ ray, and radio emission, CMEs and energetic particle production.

The Deep River neutron monitor rate (daily averages) shows multiple decreases in both March and June, with the June levels being the lowest ever recorded [*Webber and Lockwood*, 1993]. The 9 months of neutron monitor data plotted in Figure 2 illustrate several different facets of cosmic ray modulation: the first 3 months reflect the recovery phase of the 11-year modulation cycle; the sharp decreases, with their rapid partial recovery produced by strong interplanetary shocks in March, June, and July, are prime examples of Forbush decreases; and there is a net decrease in the monitor counting rate of $\sim 11\%$ between February and August that can be ascribed to the longer-term effect of the GMIR.

At 1 AU there are more than 30 solar energetic particle events over the 12-month period (Figure 3) starting in late November 1990 with a distinct clustering of events at the lower energies over the March through mid-July time period

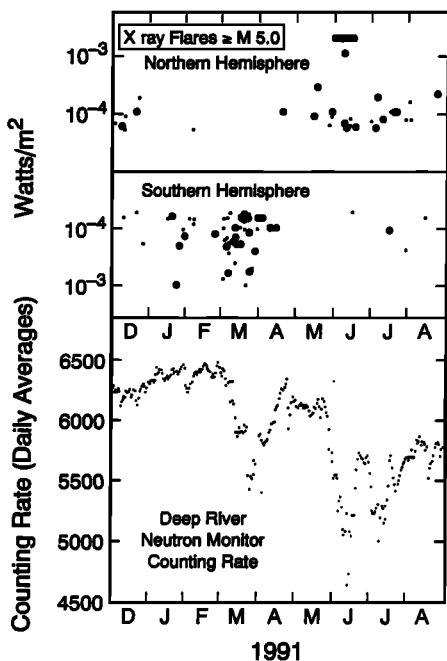


Figure 2. The top two panels mark the time of occurrence of X ray flares $\geq M 5.0$ as a function of X ray intensity. Flares that occurred in the northern hemisphere are in the top panel, and those in the southern hemisphere are plotted in the center panel. Note that the energy scale has been inverted for flares in the southern hemisphere. The encircled points were flares accompanied by a coronal mass ejection (all data from the NOAA Solar-Geophysical Bulletin).

consistent with the formation of what *Dröge et al.* [1992] have termed super events.

All of these 1 AU observations are significantly influenced by the relative separation in heliolongitude between the Earth and the site of the solar activity. The observed size of solar cosmic ray increases and Forbush decreases are strong functions of this relative separation. The effects of some of the most intense CMEs that could have occurred on the back side of the Sun would not be directly observed at Earth.

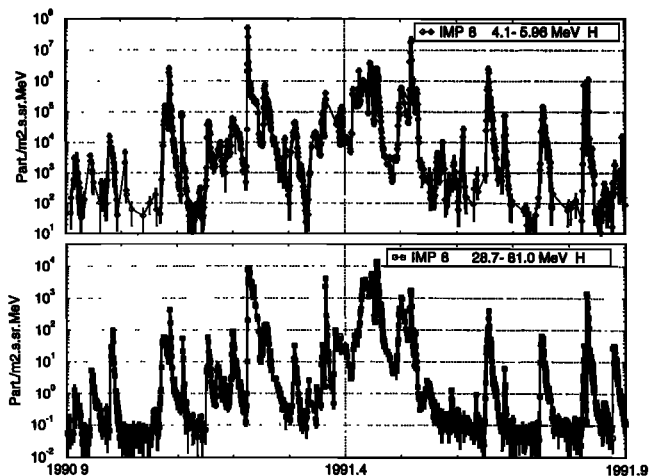


Figure 3. Time history (6 hour averages) of 4–6 and 28–60 MeV H from the GSF C IMP 8 experiment (R. McGuire, Principal Investigator (PI) at 1 AU.

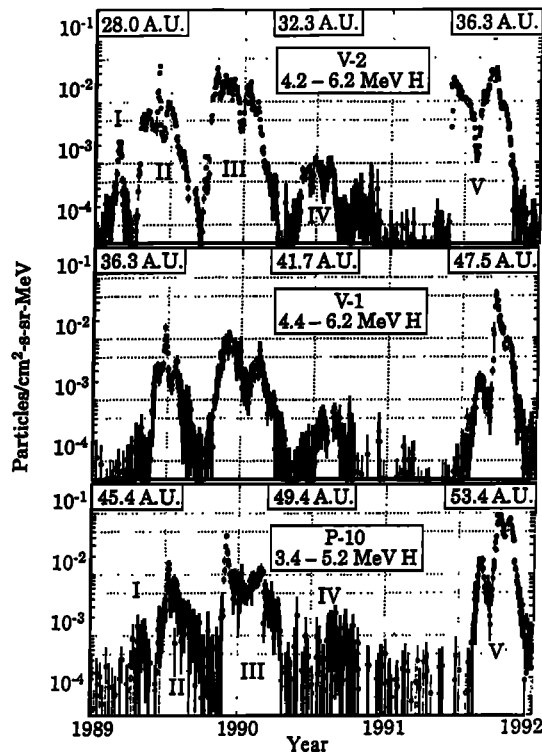


Figure 4. Time history (24 hour averages) of low-energy protons from the CRS experiment on Voyagers 1 and 2 (E. Stone, PI) and the P10 CRT experiment (F. McDonald, PI) for the period of maximum solar activity of cycle 22.

2.3. Overview of the Pioneer and Voyager Energetic Particle Observations

The time history of MeV protons at heliocentric distances greater than 25 AU (Figure 4) for the 1989–1992 cycle 22 period of high solar activity shows that the large number of CMEs and their associated solar energetic particle events observed at 1 AU have merged to form 5 long-lived solar/interplanetary (S/IP) events. In a preliminary study, *McDonald and Selesnick* [1991] found the following general properties for the first four events: they were associated with periods of strong solar activity; were convected radially outward with the solar wind velocity; their radial intensity gradients in the outer heliosphere were in the range -8 to $-14\%/AU$ (neglecting longitudinal effects); there were no systematic latitudinal gradients up to $\lambda = 32^\circ$, and their energy spectra were characterized by exponentials in rigidity but with different values of R_0 for H and He. *McDonald et al.* [1993] found that events II, III, and IV were closely associated with major step decreases in the cosmic ray intensity.

Despite their increasing heliocentric distances the 1991 V1 and P10 energetic particle events are about a factor of 5 larger than those observed earlier in the cycle while the V2 intensity is comparable to the peak value of event 3 (Figure 4). As viewed in the context of MeV ions, the 1991 event was the largest observed in the outer heliosphere over the past two solar cycles (extrapolating to earlier times, that is, smaller heliocentric distances, assuming a radial intensity gradient of $-10\%/AU$).

The intensity profiles of MeV ions for the 1991 event at

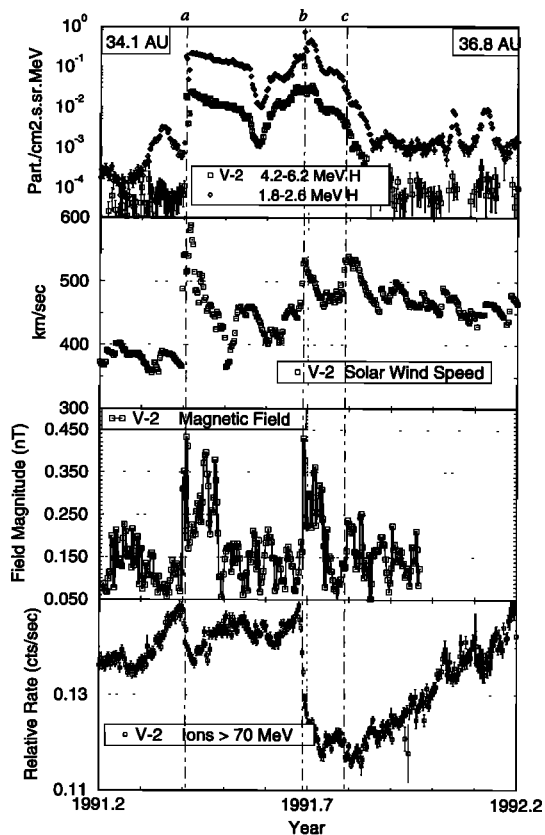


Figure 5. Time history of V2 (24 hour averages) 1.8–2.6 MeV and 4.2–6.2 MeV H along with the daily averages of the solar wind speed (from the V2 Solar Wind experiment, J. Belcher, PI), the magnitude of the interplanetary magnetic field (N. Ness, PI) and the counting rate of galactic cosmic rays with energies >70 MeV from the CRS experiment. The three vertical lines mark the passage of the three major peaks in the solar wind speed over this period and are the main fiducial marks for the analysis of this event.

V2, V1, and P10 are very similar, with a double-peak structure produced by the two episodes of solar activity. There are, however, important differences that will be covered in the following discussion of the data from the individual spacecraft.

Voyager 2: The dominance of the interplanetary disturbances over the MeV particles is evident in the combined plot of the solar wind speed V_{sw} ; the magnitude of the interplanetary magnetic field B ; the flux of 1.8–2.6 and of 4.2–6.2 MeV H and the intensity of galactic cosmic ray ions >70 MeV (Figure 5). While there is a small particle precursor at the lowest energy, the onset of the GMIR is clearly marked by the simultaneous sharp increase in V_{sw} and B on day 146 followed by a rapid increase in the intensity of MeV ions some 1.25 days later as previously noted by *Selesnick et al.* [1991]. The three most significant peaks in V_{sw} and B are indicated by the vertical lines extending across all four data sets. The peaks in the particle intensity are associated with these interplanetary disturbances. There are several instances where there is a strong correlation between decreases in the solar wind speed and in the intensity of MeV ions. The small increases of 1.8–2.2 MeV protons at 1992.05 and 1992.12 are probably produced by

corrotating interaction regions (CIRs). An earlier CIR could also have been the source of the “precursor” event at 1991.35. The effects of the interplanetary disturbances on the galactic cosmic ray intensity will be discussed in a later section in conjunction with the V1 and P10 data.

While the onset and duration of this event at V2 is essentially identical for 30–56 MeV H and 4–6 MeV H (Figure 6), there are significant differences between the time histories of the higher- and lower-energy ions of solar/interplanetary origin. For 30–56 MeV H peak b intensity is almost an order of magnitude larger than the peak a while for 4–6 MeV H there is only 25% difference. At the higher energy the maximum intensity occurs just before the plasma peak speed (b) but just behind it at lower energies. Furthermore, the valley separating peaks a and b occurs much earlier (~50 days) at the higher energies than at the lower energies. There is a distinct increase in the flux of 2.5–8.8 MeV electrons that rises above the background levels some 24 days before peak b with a rapid decrease following the passage of this peak speed region (Figure 6). The time history of these electrons is not unlike that of the 30–56 MeV H.

Pioneer 10: Beyond 50 AU at P10, there is also a close correspondence between the profile of changes in the solar wind speed and the time history of 3.4–5.2 MeV H (Figure 7). The three principal peaks in the P10 solar wind speed have been labeled a, b, and c. These designations are used as guides in the comparison of the data from the three spacecraft and probably represent similar intervals of enhanced solar activity rather than specific solar events. The near

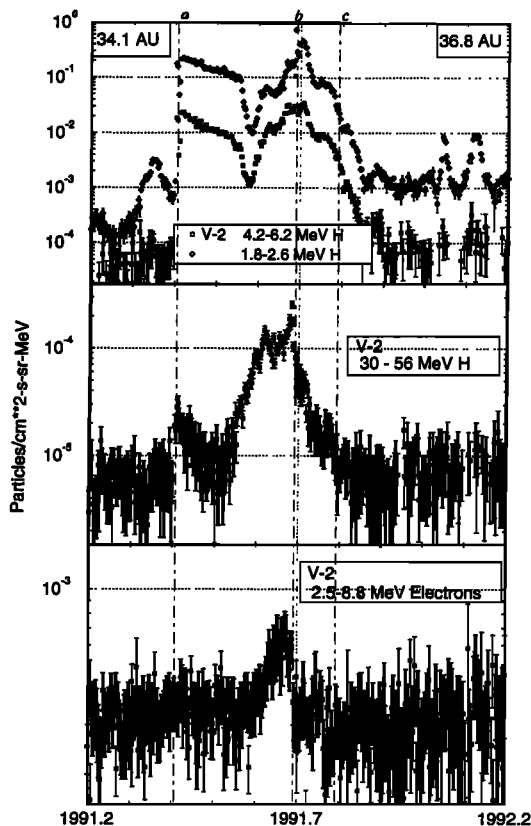


Figure 6. Time history at V2 (24 hour averages) of low-energy H, 30–56 MeV H and 2.5–8.8 MeV electrons.

coincidence between the two major peaks (b and c) in the solar wind speed with maxima in the energetic particle intensity is very similar to that observed at V2 except at P10 the peaks in the energetic particle intensity precede those in the plasma speed. The more modest increase in the solar wind speed at peak a is reflected in the smaller increase in the MeV ion intensity relative to the b peak.

Voyager 1: There are no data on the interplanetary medium available at V1 at this time so the low-energy ion observations are used for the identification of the three peaks based on similarities with the V2 and P10 data (Figure 8). At $\lambda = 32^\circ\text{N}$ the Voyager 1 MeV ion intensity for the a peak is an order of magnitude smaller and the risetime is much longer than observed at V2. Peak b intensity at V1 is comparable with that of V2, but the risetime at V1 is much more rapid than the risetime for V2. These differences in the V1/V2 response are most naturally explained by their differences in latitude with respect to that of the solar activity. The March solar activity was in the southern hemisphere of the Sun at solar latitudes of $20^\circ\text{--}25^\circ$ with V1 at 32°N and V2 at 6°S , while the June flares were located close to the heliollatitude of V1.

The 30–56 MeV ions at V1 (Figure 8) have a single relatively sharp peak that resembles a 1 AU energetic storm particle event except on a timescale of days instead of hours. This analogy suggests that these higher-energy particles are produced by the interaction of the ambient MeV ions with the strong shock implied by both peak b and the response of the integral intensity of galactic cosmic rays >70 MeV.

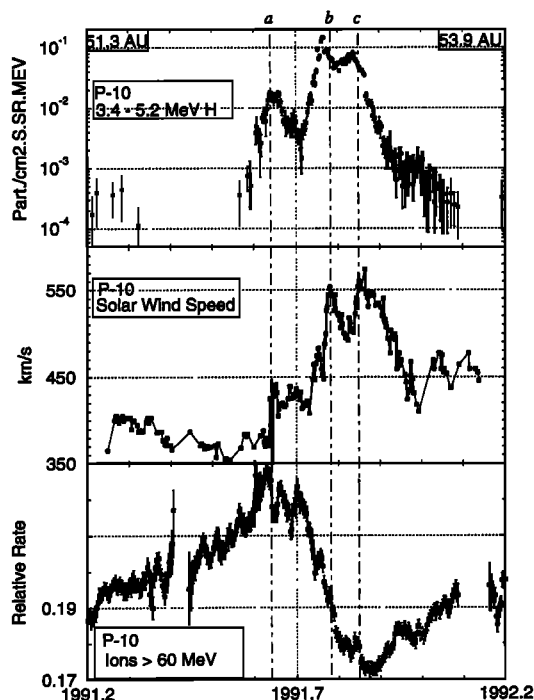


Figure 7. Time history of P10 (24 hour averages) 3.5–5.2 MeV H, along with the solar wind speed (from the P10 Ames plasma analyzer. (A. Barnes, PI) and the integral intensity of ions >56 MeV. The choice of the three peaks in the solar wind data (indicated by vertical lines) is based on their apparent correspondence to the V2 data. These V2 and P10 peaks probably reflect the same intervals of solar activity rather than specific events.

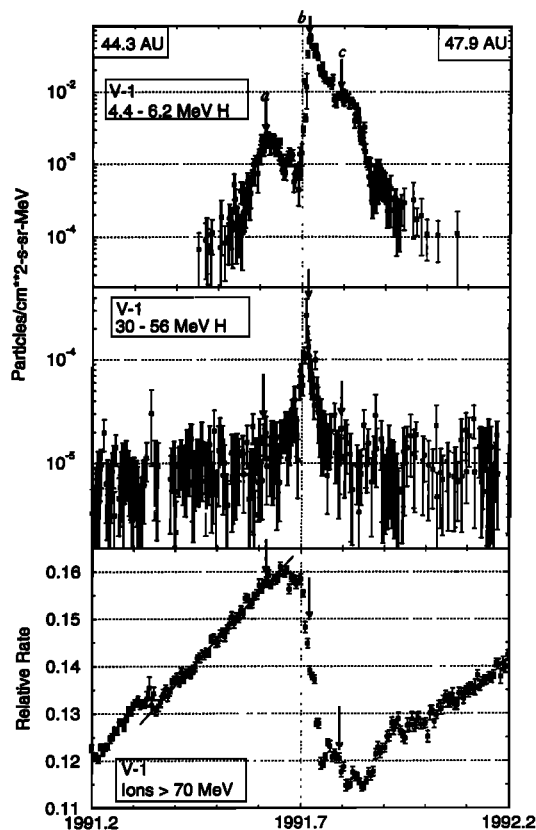


Figure 8. Time history at V1 (24 hour averages) of 4.4–6.2 MeV H, 30–56 MeV H and the counting rate of the galactic cosmic rays >70 MeV. The arrows mark the chosen location of the a, b and c peaks based on correspondence with the V2 and P10 low-energy ion data.

There was no statistically significant increase in the flux of 2–8 MeV electrons observed at V1.

2.4. Energy Spectra and Radial Intensity Gradients

The momentum spectra for H and He over the three peak periods for the three spacecraft are shown in Figures 9–11. Such spectral measurements provide information on the acceleration process, while the H/He ratio provide insight on the source region for these ions. Above rigidities of 200–300 MV significance fluxes of anomalous helium and galactic cosmic ray protons are present so the spectral studies are limited to 1.8–8.2 MeV/nucleon region. These data are not consistent with a power law in kinetic energy but can be fit by a number of other functional forms such as exponentials in energy, energy/charge, rigidity, and momentum/nucleon. Most of these were discarded because of the greater difference in the characteristic values of E_0 , E_{0q} and R_0 for H and He.

The values of P_0 for H and He and the H/He ratio for the data shown in Figures 9–11 are summarized in Table 1. This analysis suggests that the spectra appear to harden somewhat with increasing heliocentric distance. For peak b the H and He intensities from 2–70 MeV/nucleon are remarkably similar at all three spacecraft (Figure 10) over the complete energy range despite their great separation in space. For peak c the respective H and He intensities at V1 and V2 are again essentially identical but at 4 MeV are about a factor of

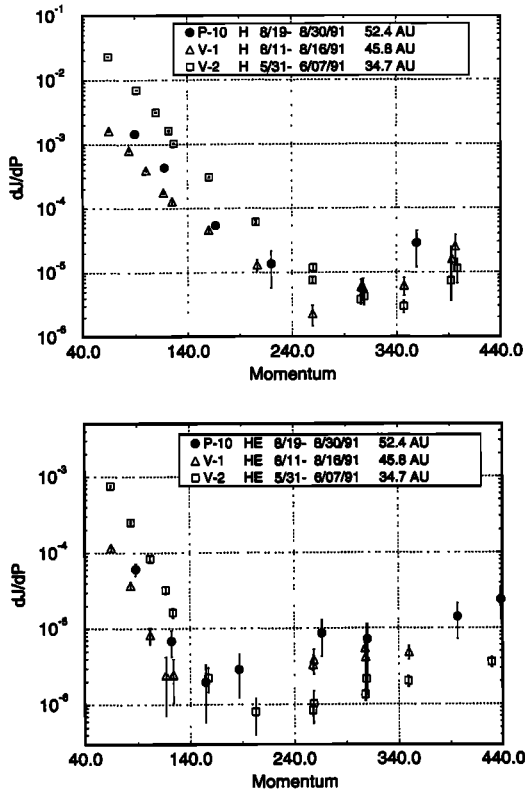


Figure 9. H and He momentum/nucleon spectra for time intervals at the three spacecraft in the outer heliosphere centered about the a peak.

2 smaller than observed at P10. It should also be noted that at peak b the ratio of $(P_0)_{\text{He}}/(P_0)_{\text{H}} \approx 1$ and is close to 1 for peak c at both V1 and P10, and at V2 is equal to 1 just after the c peak (see Figure 12).

To examine the spectral variation, the values of P_0 and E_{0p} (based on an exponential in total energy/charge) have been plotted (Figure 12) for some 19 time intervals that span the complete event at V2 (for He, $(R_0)_{\text{He}} = 2(P_0)_{\text{He}}$). Also shown for the same time intervals is the H/He ratio for 1.8–2.8 MeV/nucleon ions. This analysis indicates that a spectral fit of the form $J_0 \exp(-P/P_0)$ (where P is the momentum/nucleon) is superior in the region of peaks b and c (Table 1, Figure 12) in that the values of P_0 for H and He are more nearly the same. However, no single representation was found to be adequate over the entire event. The small value of the H/He ratio = 25.3 and its limited variation over the event (except in the vicinity of the intensity minimum between the a and b peak) more closely resemble those of CIR-associated particle events [Van Hollebeke *et al.*, 1978; McGuire *et al.*, 1978; Mewaldt *et al.*, 1979].

For peak a there is a -7.5% AU radial intensity gradient for 4 MeV ions between V2 and P10. The significantly lower intensity at V1 compared to P10 is indicative of a negative latitudinal gradient with $G_\lambda = -3.5\%/deg$. Such measurements of G_r and G_λ should be regarded with caution because of heliolongitude effects and the particular difficulty of identifying the proper time interval at the three spacecraft for this period. For peak b the radial (34–50 AU) and latitudinal gradients measured at the three spacecraft are zero, while the c peak requires a positive radial gradient. The

most logical explanation for such apparent gradients is in terms of a significant variation of intensity with heliolongitude combined with the match between the heliolatitude of V1 and the June flare activity.

While the radial gradient inferred between the three spacecraft does not yield a consistent picture, an intensity gradient of $-24\%/AU$ is obtained between 1 and 35 AU by comparing the average flux of 5 MeV ions at Voyager 2 over the 1991.65–1991.75 time period with that observed at 1 AU averaged over the period 1991.4–1991.47. This value is comparable to the value of $-45\%/AU$ between 1 and 10 AU and $-15\%/AU$ from 10–30 AU for 11–21 MeV ions measured by Dröge *et al.* [1992] for a series of earlier S/IP events.

2.5. Changes in the Galactic Cosmic Ray Intensity

The integral rate of galactic cosmic ray intensity for ions >70 MeV shown in Figures 5, 7, and 8 is the same data set as that used by Webber and Lockwood [1993] in their studies of the changes in cosmic ray intensity associated with the 1991 activity. They find decreases of 21%, 28.3%, and 20.5% at V2, V1, and P10 respectively with a much slower rate of decrease at P10. The overall changes at P11 [Van Allen and Fillius, 1992] were very similar to that at V2.

These cosmic ray decreases at 1 AU and in the outer heliosphere occur at a time when a strong recovery was underway from the low-intensity level of the solar maximum period. The passage of the peak a disturbance interrupts this recovery of galactic cosmic rays at V2, P10, and P11 but appears to have no effect at V1. These relative changes become more apparent when the normalized V1 and V2

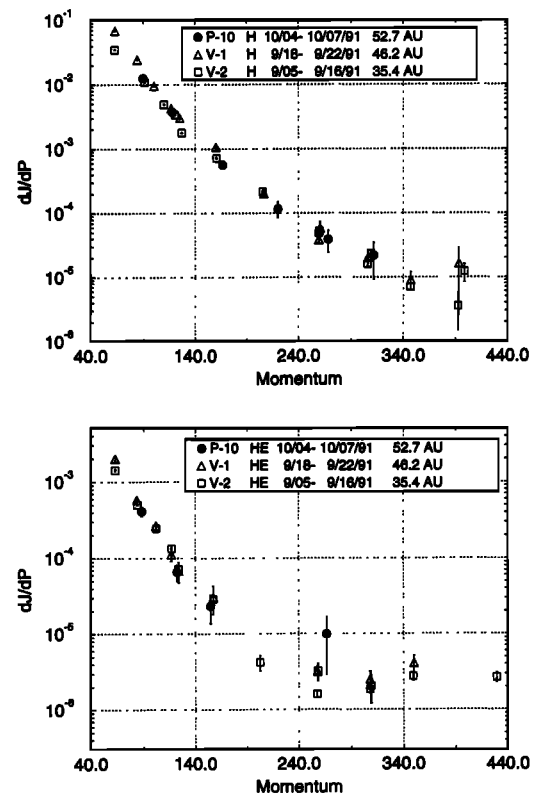


Figure 10. H and He momentum/nucleon spectra for time intervals at the three spacecraft centered about the b peak.

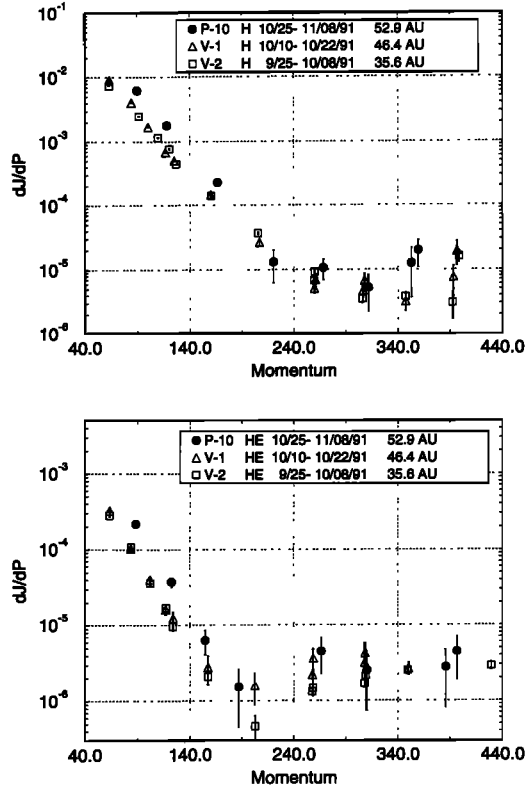


Figure 11. H and He momentum/nucleon spectra for time intervals at the three spacecraft centered about the c peak.

integral rates over this period are compared (Figure 13). Assuming the recovery is the result of changes in the outer heliosphere beyond the two spacecraft, the V1/V2 comparison suggest that peak a decrease at V2 would have been much larger in the absence of an ongoing recovery. This supposition is illustrated qualitatively by the dashed line in Figure 13 under the assumption that the recovery rate at V2 is the same as at V1.

The integral rates at V1 and V2 were comparable both at the beginning of 1991 and after the passage of peaks b and c disturbances as well as during the ensuing recovery period while the magnitude of the decrease observed at P10, P11, and V2 was essentially the same [Van Allen and Fillius, 1992; Webber and Lockwood, 1993]. Thus the net effect of

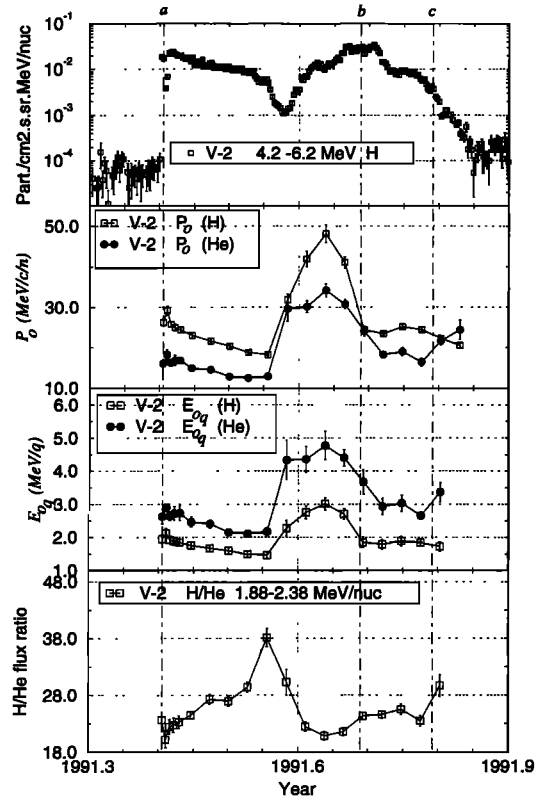


Figure 12. The characteristic values P_0 and E_{0q} obtained by fitting the V2 data as an exponential in momentum/nucleon (i.e., proportional to particle velocity at these energies) and as an exponential in total kinetic energy charge. The averages are generally taken over a 10-day interval. Also shown for reference is the time history of 4.2–6.2 MeV H and the H/He ratio for 1.9–2.4 MeV/nucleon ions. The vertical lines mark the location of the a, b, and c peaks as defined in Figure 5.

the GMIR on the galactic cosmic ray intensity was the same at all of the four locations in the outer heliosphere.

2.6. Relation of Solar Events to Pioneer/Voyager Observations

The ecliptic plane projections of the locations of P10 and V1 and V2 are shown in Figure 14 for March 1991 along with the arcs described by Earth, Pioneer Venus Orbiter (PVO),

Table 1. Values of P_0 for Spectral Fits of the Form Exponential

	Time Interval	AU	$(P_0)_H$	$(P_0)_{He}$	$(P_0)_{He}/(P_0)_H$	H/He
				<i>Peak a</i>		
V2	May 31 to June 7, 1991	34.7	24.9 ± 0.7	16.7 ± 0.3	0.67 ± 0.03	23.8 ± 0.8 (1.9–2.4 MeV/nucleon)
V1	Aug. 11–16, 1991	45.8	24.1 ± 2.0	14.0 ± 1	0.58 ± 0.07	12 ± 1.7 (1.9–2.4 MeV/nucleon)
P10	Aug. 19–30, 1991	52.4	26.4 ± 0.7	18.6 ± 3	0.70 ± 0.11	21.9 ± 4 (3.4–4.9 MeV/nucleon)
				<i>Peak b</i>		
V2	Sept. 5–16, 1991	35.4	23.9 ± 0.6	23.2 ± 1.2	0.97 ± 0.06	24.5 ± 0.6
V1	Sept. 18–22, 1991	46.2	18.6 ± 1	19.2 ± 1.5	1.03 ± 0.1	34.4 ± 3
P10	Oct. 4–7, 1991	52.7	29.0 ± 3.0	25.1 ± 5	0.87 ± 0.2	28.6 ± 4
				<i>Peak c</i>		
V2	Sept. 25 to Oct. 8, 1991	35.6	25.0 ± 0.4	18.9 ± 0.4	0.76 ± 0.03	26.5 ± 1
V1	Oct. 10–22, 1991	46.4	20.1 ± 1.5	18.2 ± 1.5	0.91 ± 0.1	28.0 ± 2
P10	Oct. 25 to Nov. 8, 1991	52.9	26.8 ± 1.6	26 ± 4	0.97 ± 0.15	27/3 ± 2

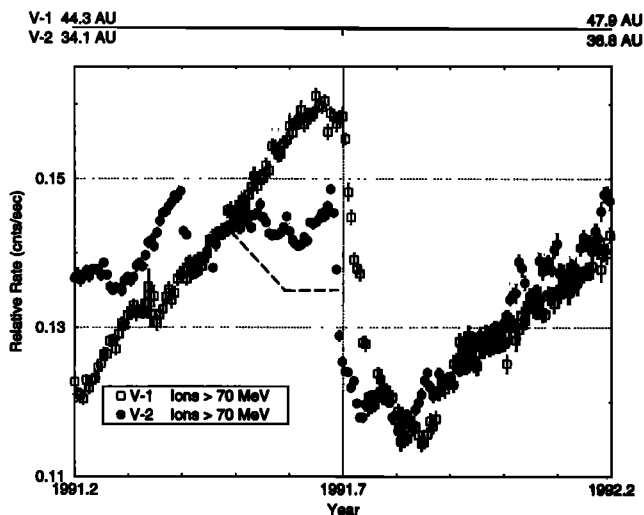


Figure 13. A comparison of the normalized V1 and V2 H rates (galactic cosmic rays >70 MeV). The heavy dashed line is an estimate of the decrease that would have been observed at V2 in the absence of an ongoing recovery at greater heliocentric distances.

and Ulysses during this month. The dashed arrows mark the heliolongitude of the some 14 M-5 or larger flares observed from Earth that had associated CMEs. At this time the relative position of the three monitoring platforms in the inner solar system is biased in favor of observing events directed toward P10.

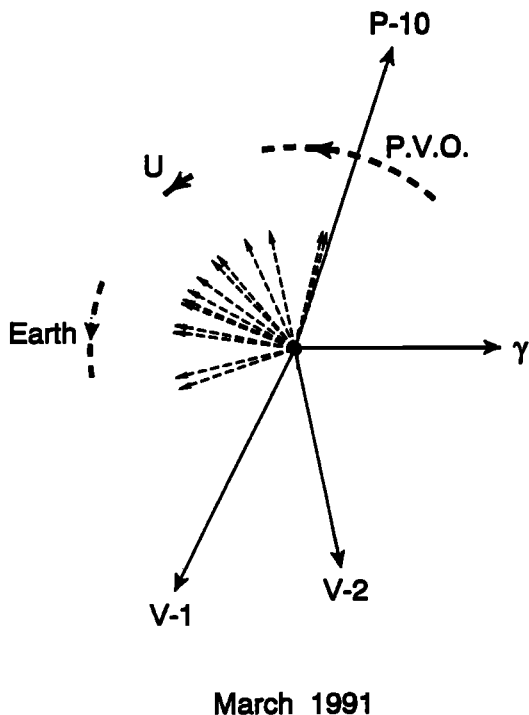


Figure 14. The ecliptic projection of the location of P10 and V1/2 are plotted for March 1991 along with the arcs described by Earth, Pioneer Venus orbits and Ulysses during this month. The heliolongitude of the M-5 or larger flares with coronal mass ejections are indicated by the dashed arrows.

On March 12 there was a sharp increase in the solar wind speed to ≈ 850 km/s as observed by the Ames Plasma Experiment on PVO. This increase in V_{sw} is most probably associated with the flare activity in region 6545 that began on March 12. At P10 the first significant change in plasma speed occurs on day 232 with V_{sw} increasing from 371 to 424 km/s. Using these two time markers to estimate the approximate time for the March activity to propagate out to 52.5 AU gives an average velocity of 573 km/s. While this velocity is consistent with the 0.8 and 52.5 AU observations it also implies considerable deceleration as these disturbances propagate out from the Sun.

At Voyager 2 the initial increase in V_{sw} and B occurred on day 146 at 34.6 AU with a peak value of $V_{sw} = 590$ km/s on day 150. The CMEs that produced this disturbance most probably originated on the back side of the Sun, possibly associated with region 6538 in late February 1991. The relative position of peak a at P10 and V1 with respect to the intensity minimum is very different from that of V2 suggesting there is not a straightforward correlation between the three spacecraft for this peak.

Figure 15 gives a projection for June 1991 identical to that of Figure 14 except that only the location of the six flares that were X-10 or larger are shown. At this time the V1 and V2 spacecraft are more nearly aligned with Earth and the observed solar activity. The Ames PVO solar wind experiment observed values of $V_{sw} \sim 1100$ km/s on May 31 and 1230 km/s (near saturation) on June 6 with the latter probably in association with the June 6 X-12 event. The sharp decreases in the earth-based neutron monitor counting rates on May 31, June 4, and June 12 mark the passage of strong interplanetary shocks. At V2 the plasma speed increased from 462 to 529 km/s between day 250 and day 252. Since all

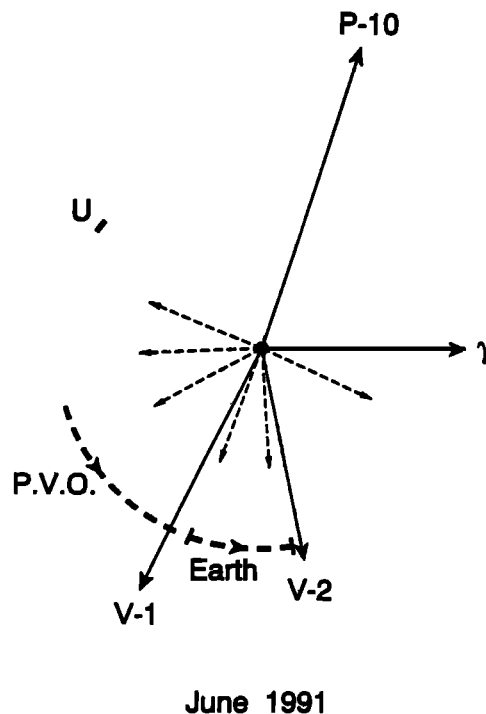


Figure 15. Same for Figure 14 except covering June 1991 and only the heliolongitude of the 6 X-10 or larger flares are plotted.

of the large June events probably contributed to the b peak, the mean start time is taken as June 7, giving an average transit velocity of 650 km/s to V2 and 774 km/s to V1.

At P10 (whose heliocentric distance is 6.8 and 17 AU greater than V1 and V2 with a separation in heliolongitude of 170° from V1), peak b is observed on day 284 with a peak speed $V_{sw} = 553$ km/s. The essentially identical intensities at the three spacecraft argue that region 6659 produced one or more CMEs in late May that were even stronger than those observed in June from the visible side of the disc.

Of course the same argument must be evoked for peak c where the P10 MeV ion intensities are twice as large as those at the Voyagers. The approximate 26-day separation between peaks b and c at P10 provides added consistency to the argument that one or more exceptional backside events occurred in the latter half of June.

3. Discussion

In the outer heliosphere the MeV ions define an event that extends over a 6-month period and whose time profile is controlled by the passage of interplanetary disturbances. The geneses of these disturbances, the coronal mass ejections of March and June 1991 and adjacent time periods, were in some cases the sources of large fluxes of solar energetic particles. The key question then arises: are the ions and electrons observed some 5 months later in the outer heliosphere the solar energetic particles accelerated in the inner heliosphere and continually reenergized by the shocks within the GMIR or are they more recently accelerated by these shocks from a seed population of superthermal solar wind ions? There must be contributions from both processes but establishing the relative proportions will require detailed modelling of the event.

The shape of the observed energy spectra is determined by the shock parameters and the processes that remove particles from the acceleration region. With an essentially azimuthal interplanetary magnetic field and with multiple CMEs filling most of the near equatorial region, adiabatic energy losses should become the dominant loss process. *Fisk and Lee* [1980] have considered such a model for shock acceleration in co-rotating interaction regions under the assumption that the diffusion coefficient K_r is of the form $K_r = vg(r) = K_0vr$ at heliocentric distances $\leq \sim 5$ AU where K_0 is a constant, v is the particle velocity, and r is the heliocentric distance. This leads to a spectral form $\exp - [6K_0v/V_{sw}]f(\beta)$ (where $f(\beta)$ is a function of the shock parameters) which is in agreement with the relative values of $(P_0)_H$ and $(P_0)_{He}$ in Table 1 and Figure 12 for the spatial region near the b and c shocks.

A ratio of $B/B' = 0.2$ (where B and B' are the upstream and downstream values of the interplanetary magnetic field) and $P_0 = 24$ MeV/nucleon gives a value of the scattering mean free path $\lambda = 0.1$ AU at 1 AU and 3.5 AU at 35 AU. The 1 AU value of λ is consistent with *Palmer's* [1982] summary of the observational data.

For corotating events between 1 and 5 AU, *McDonald et al.* [1976], *Van Hollebeke et al.* [1979], *McGuire et al.* [1978], and *Mewaldt et al.* [1979] found that the spectra were well fit by an exponential in rigidity. At 1 AU, *Mewaldt et al.* found there was considerable variation in R_0 , but the ratio of $(R_0)_{He}/(R_0)_H$ remained relatively constant near 1.5 ± 0.1 ($=0.75$ for $(P_0)_{He}/(P_0)_H$). However, *Gloeckler et al.* [1979],

in a study of three events, found that the distribution function of H, He, C, N, O, and Fe had an exponential dependence on the particle speed, v , from 0.15 to 8 MeV using data from IMP 8. This apparent discrepancy has not been resolved and may reflect the different energy intervals and time periods used in the various studies. At V2, $(P_0)_{He}/(P_0)_H \approx 0.77$ during the initial half of the event. These spectral features as well as the H/He ratio of 25.3 at 2 MeV/nucleon are very similar to those observed in CIR events in the inner heliosphere [*Van Hollebeke et al.*, 1978; *McGuire et al.*, 1978; *Mewaldt et al.*, 1979], where *McGuire et al.* measured a H/He ratio of 22 ± 5 . In a recent study of 1-4 MeV/nucleon solar energetic particles, *Reames* [1992] found a weighted mean average for H/He of 21.1 ± 1.6 with a much smaller variation between events than had been observed previously at higher energies. From the present analysis it is not possible to establish the origin of the MeV ions in the outer heliosphere. However, the ongoing acceleration is consistent with shock acceleration with adiabatic deceleration as the principal loss process.

The presence of 2-8 MeV electrons poses a major problem for these interplanetary shock processes if they are to be accelerated from the solar wind. *Lopate* [1989] has used the P10/11 data from 7 to 28 AU to study the acceleration of 2-7 MeV electrons and 11-20 MeV/nucleon ions and concludes that separate mechanisms are necessary for these two components: shock drift processes for the 11-20 MeV/nucleon ions and a two-step Fermi process for the electrons. However, on the basis of the similarities of the 30-56 MeV H and 2-8 MeV electrons time histories (Figure 6) for the June event and especially for the large 1989 electron and ion event [*McDonald and Selesnick*, 1991], this electron component may simply be a minute fraction of the original solar flare electrons that is "maintained" by the GMIR. These electrons are decreasing rapidly in intensity with increasing heliocentric distance at a faster rate than the ion component as evidenced by the fact that electrons were not seen above background with an identical detector system at V1, while the ion intensity at the two spacecraft were at comparable levels. It should be noted that the largest increase in MeV electrons in the outer heliosphere was reported by *Pyle et al.* [1984] at 28 AU in association with the June 1982 events. For the June 3, 1982, event *McDonald and van Hollebeke* [1985] reported 2-6 MeV electron fluxes at 0.5 AU equal to the H intensity at the same energy. The MeV electrons in the heliosphere may then be just a few stragglers from the ultrarich electron events that have been reaccelerated by the GMIR.

The association of the decreasing plasma velocity and MeV ions intensity at the end of the March and June episodes suggest that this superposition of multiple post-shock regions may be an important feature of the GMIR. *Pyle et al.* [1984] made a similar point about the 1982 event, and in our preliminary studies we have found this to be one of the characteristics of GMIRs associated with step decreases in the cosmic ray intensity.

The GMIR associated with the March/June 1991 activity reduced the >70 MeV galactic cosmic ray rate at V1/2 and P10 to their lowest level in cycle 22. Furthermore, despite the strong latitudinal asymmetry in the observed solar activity, this decrease is effectively the same at all four spacecraft in the outer heliosphere.

This GMIR appears to be the most logical trigger for the

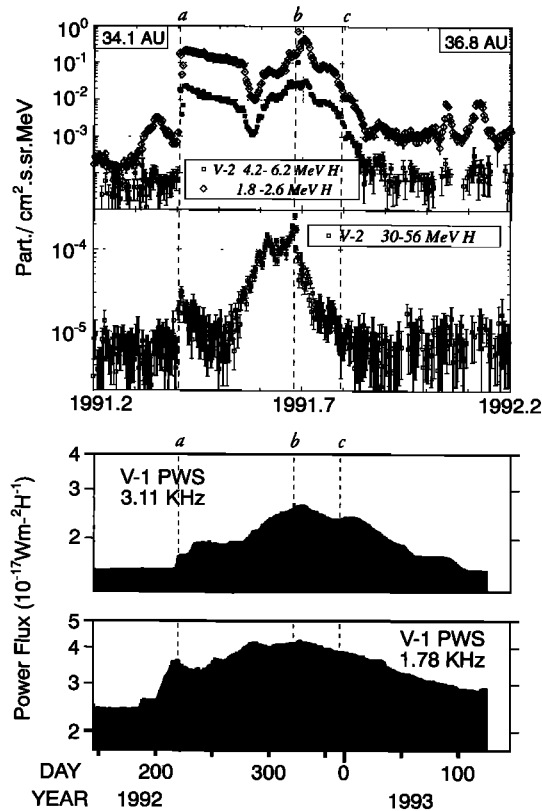


Figure 16. A comparison of the time history of low- and medium-energy S/IP ions at V2 and the low-frequency radio emission detected at V1 and V2 [Gurnett et al., 1993] starting on day 209, 1992. A time delay of 1.2 years is used to align the a peak with the onset of the first plateau in the 3.11-KHz emission.

long-duration, low-frequency radio noise detected at V1 and V2 starting on D209, 1992 by the Voyager Plasma Wave Experiment (PWS) [Gurnett et al., 1993]. The time history of this radio emission (Figure 16) shows a remarkable resemblance to that of the low-energy ions when a time delay of 1.2 years is introduced. This delay was adopted to line up the particle peak a at V2 with the initial plateau of the 3.11-kHz radio emission. While this choice of delay times is not unique, it is clear that a time shift of this order will bring the two data sets into general alignment. While the GMIR structure will continue to evolve over such a lengthy period, it is interesting to note that features corresponding to peaks b and c can be found in the 3.11-kHz data. The concept of a solar wind “trigger” for these low-frequency rapid emissions was first advanced by McNutt [1988] to explain the 1983/1984 PWS observations [Kurth et al., 1984]. The concept of a GMIR as the driving force for these events represents an extension of McNutt’s original hypothesis.

The PWS investigators have proposed that a possible source for this emission is the interaction of shock waves with the enhanced plasma density in the region of the nose of the heliopause beyond the termination shock [Gurnett et al., 1993]. The extended temporal duration of the MeV ion event in the outer heliosphere and the energy available from the superposition of multiple CMEs make this largest GMIR of the last two solar cycles an attractive candidate for produc-

ing the strongest radio emission yet observed in the outer heliosphere by the Voyager PWS.

Such a correlation between GMIRs and the low-frequency radio events gives a time delay of 1.46 years between the solar events and the onset of the radio emission and would establish the long lifetimes required if GMIRs are to be the dominant cause of the 11-year modulation.

Acknowledgments. The authors wish to express their appreciation to J. Belcher and A. Lazarus of the MIT Voyager Plasma Science Experiment for making the 1991 Voyager solar wind data available to us. We are indebted to M. A. Lee and Vladimir Ptuskin for discussions on diffusive shock acceleration and we thank Pam Schuster for her data analysis and graphics support.

The Editor thanks a referee for his assistance in evaluating this paper.

References

- Burlaga, L. F., F. B. McDonald, N. F. Ness, R. Schwenn, A. J. Lazarus, and F. Mariani, Interplanetary flow systems associated with cosmic ray modulation in 1977–1980, *J. Geophys. Res.*, **89**, 6579, 1984.
- Burlaga, L. F., F. B. McDonald, M. L. Goldstein, and A. J. Lazarus, Cosmic ray modulation and turbulent interaction regions near 11 AU, *J. Geophys. Res.*, **90**, 12,027, 1985.
- Burlaga, L. F., F. B. McDonald, N. F. Ness, and A. J. Lazarus, Cosmic ray modulation: Voyager 2 observations, 1987–1988, *J. Geophys. Res.*, **96**, 3789, 1991.
- Burlaga, L. F., F. B. McDonald, and N. F. Ness, Cosmic ray modulation and the distant heliospheric magnetic field: Voyager 1 and 2 observations from 1986 to 1989, *J. Geophys. Res.*, **93**, 1, 1993.
- Decker, R. B., R. E. Gold, and S. M. Krimigis, Distribution of 30–4000 KeV ions associated with an interplanetary shock at Voyager 2 (30 AU) and Voyager 1 (38 AU) in 1989, *Proc. 22nd Int’l Cosmic Ray Conf. (Dublin)*, **3**, 296, 1991.
- Dröge, W., R. Müller-Mellin, and E. W. Cliver, Superevents: their origin and propagation through the heliosphere from 0.3–35 AU, *Astrophys. J.*, **387**, L97, 1992.
- Fisk, L. A., and M. A. Lee, Shock acceleration of energetic particles in corotating interaction regions in the solar wind, *Astrophys. J.*, **237**, 620, 1980.
- Gloeckler, G., D. Hovestadt, and L. A. Fisk, Observed distribution functions of H, He, C, O, and Fe in corotating energetic particle streams: Implications for interplanetary acceleration and propagation, *Astrophys. J. Lett.*, **230**, L191, 1979.
- Gosling, J. T., The solar flare myth, *J. Geophys. Res.*, **98**, 18,937, 1993.
- Gurnett, D. A., W. S. Kurth, S. C. Allendorf, and R. L. Poyntner, Radio emission from the heliopause triggered by an interplanetary shock, *Science*, **262**, 199, 1993.
- Kahler, S., Solar flares and coronal mass ejections, *Ann. Rev. Astron. Astrophys.*, **30**, 113, 1992.
- Kurth, W. S., D. A. Gurnett, F. L. Scarf, and R. L. Poyntner, Detection of a radio emission at 3 KHz in the outer heliosphere, *Nature*, **312**, 27, 1984.
- le Roux, J. A., and M. S. Potgieter, The simulation of merged interaction regions in the outer heliosphere, *Adv. Space Res.*, **13**, 251, 1993.
- Lopate, C., Electron acceleration to relativistic energies by traveling interplanetary shocks, *J. Geophys. Res.*, **94**, 9995–10,010, 1989.
- McDonald, F. B., and R. S. Selesnick, Solar interplanetary energetic particles in the outer heliosphere, *Proc. 22nd Int’l Cosmic Ray Conf. (Dublin)*, **3**, 189–192, 1991.
- McDonald, F. B., and M. A. I. van Hollebeke, Solar energetic particle observations of the 3 June 1982 and 21 June 1980 gamma ray neutron events, *Astrophys. J. Suppl.*, **73**, June 1990.
- McDonald, F. B., B. J. Teegarden, J. H. Trainor, T. T. von Roseninge, and W. R. Webber, The interplanetary acceleration of energetic nucleons, *Astrophys. J. Lett.*, **203**, L149, 1976.
- McDonald, F. B., N. Lal, and R. E. McGuire, Role of drifts and

- merged interaction regions in the long-term modulation of cosmic rays, *J. Geophys. Res.*, **98**, 1243, 1993.
- McGuire, R. E., T. T. von Roseninge, and F. B. McDonald, The composition of corotating energetic particle streams, *Astrophys. J. Lett.*, **224**, L87, 1978.
- McNutt, R. L., Jr., A solar wind "trigger" for the outer heliosphere radio emissions and the distance to the terminal shock, *Geophys. Res. Lett.*, **15**, 1307, 1988.
- Mewaldt, R. A., E. C. Stone, and R. E. Vogt, Characteristics of the spectra of protons and alpha particles in recurrent events at 1 AU, *Geophys. Res. Lett.*, **6**, 589, 1979.
- Palmer, I. D., Transport coefficients of low-energy cosmic rays in interplanetary space, *Rev. Geophys. Space Phys.*, **20**, 335, 1982.
- Perko, J. S., and L. F. Burlaga, Intensity variations in the interplanetary magnetic field measured by Voyager 2 and the 11 year solar cycle modulation of galactic cosmic rays, *J. Geophys. Res.*, **97**, 4305, 1992.
- Potgieter, M. S., Time dependent modulation: Role of drifts and interaction regions, *Adv. Space Res.*, **13**, 239, 1993.
- Pyle, K. R., J. A. Simpson, A. Barnes, and J. D. Mihalov, Shock acceleration of nuclei and electrons in the heliosphere beyond 24 AU, *Astrophys. J.*, **282**, L107, 1984.
- Reames, D. V., Energetic particle observations and the abundances of elements in the solar corona, Proceedings of the First SoHo Workshop, *Eur. Space Agency Spec. Publ.*, **SP-348**, 315-323, 1992.
- Selesnick, R. S., A. C. Cummings, E. C. Stone, F. B. McDonald, and J. W. Belcher, Energetic particle and solar wind signatures in the outer heliosphere of the March 1991 solar activity, *Eos Trans. AGU*, **72(44)**, Fall Meeting suppl., 386, 1991.
- Van Allen, J. A., and R. W. Fillius, Propagation of a large Forbush decreases in cosmic-ray intensity past the earth, Pioneer 11 at 34 AU, and Pioneer 10 at 53 AU, *Geophys. Res. Lett.*, **19**, 1423, 1992.
- Van Allen, J. A., and J. D. Mihalov, Forbush decreases and particle acceleration in the outer heliosphere, *Geophys. Res. Lett.*, **17**, 761, 1990.
- Van Hollebeke, M. A. I., F. B. McDonald, J. H. Trainor, and T. T. von Roseninge, The radial variation of corotating energetic particle streams in the inner and outer solar system, *J. Geophys. Res.*, **83**, 4723, 1978.
- Webber, W. R., and J. A. Lockwood, Giant transient decreases of cosmic rays in the outer heliosphere in September 1991, *J. Geophys. Res.*, **98**, 7821, 1993.
-
- A. Barnes and J. Mihalov, Space Science Division, NASA Ames Research Center, Moffett Field, CA 94035. (e-mail: barnes@windee.arc.nasa.gov; mihalov@windee.arc.nasa.gov)
- L. F. Burlaga, Laboratory for Extraterrestrial Physics, NASA Goddard Space Flight Center, Greenbelt, MD 20771. (e-mail: u2leb@lepvax.gsfc.nasa.gov)
- P. Gazis, San Jose State University Foundation, NASA Ames Research Center, Moffett Field, CA 94035. (e-mail: hal.gazis@ames-io)
- F. B. McDonald, Institute for Physical Science and Technology, University of Maryland, College Park, MD 20742. (e-mail: fm27@umail.umd.edu)
- R. S. Selesnick, California Institute of Technology, Pasadena, CA 91125. (e-mail: rss@citsrl.srl.caltech.edu)

(Received September 7, 1993; revised April 7, 1994; accepted April 12, 1994.)